Solid State Communications, Vol. 75, No. 2, pp. 115–120, 1990.
Printed in Great Britain.

0038–1098/90 $3.00 + .00
Pergamon Press plc

MAGNETIC RESONANCE SPECTROSCOPY OF ZINC DOPED SILICON

H.E. Altink, T. Gregorkiewicz and C.A.J. Ammerlaan

Natuurkundig Laboratorium der Universiteit van Amsterdam, Valckenierstraat 65,
NL-1018 XE Amsterdam, The Netherlands

(*Received* 27 *February* 1990 *by B. Mühlschlegel*)

The spin-Hamiltonian analysis is presented of five new electron paramagnetic resonance spectra observed in silicon after indiffusion of zinc impurity. On the basis of hyperfine interactions one of the spectra is identified with a monoclinic ZnCu pair, while another spectrum arises from a trigonal ZnCr pair.

1. INTRODUCTION

ZINC IN SILICON is known to be a double-acceptor; in early investigations the ionization levels were determined from electrical resistivity and Hall effect measurements [1, 2]. Several other electrical levels in zinc doped silicon were more recently observed using transient capacitance techniques [3–5] and infrared absorption spectroscopy [6–8]. Identification of these levels with specific impurity complexes is often based on circumstantial evidence. Some of the new levels were ascribed to zinc–boron impurity pairs [5, 9] and to other zinc-acceptor pairs [1, 2]. Donor-acceptor ion-pair formation between zinc acceptors and the transition element donors iron, chromium, manganese and vanadium has been proposed on the basis of DLTS results [3]. Unambiguous evidence for the existence of the ZnMn pair was obtained from electron paramagnetic resonance [10]. Complexes so far unidentified were labelled as Zn(X1), Zn(X2) [4] or Zn(X3) [11]. Generally, the measurements on zinc doped silicon indicate the propensity of this impurity to form pairs, precipitates and complexes with residual impurities. Depending on thermal history and contaminations present only a small fraction of the zinc atoms may remain as isolated substitutional dopant. To obtain structural information on the complexes existing in zinc doped silicon electron paramagnetic resonance (EPR) spectroscopy was applied. Several hitherto unreported spectra were observed in zinc diffused silicon. Their EPR characterization will be given in this paper. For two of the spectra direct relation to zinc has already been established. These two centres are described in more detail. Observation by EPR of isolated zinc centres has previously been described in the literature [12].

2. EXPERIMENT

Samples for the experiments were prepared by diffusion of zinc into low and high resistivity silicon, both of *n*- and *p*-type. Either zinc of the natural isotopic composition or zinc enriched to 91.9% in the nuclear magnetic isotope ^{67}Zn was used. For the diffusion process silicon samples with some metallic zinc were enclosed in a quartz ampoule under argon atmosphere. No other dopants were intentionally added. Distribution of zinc through the samples was achieved by heating during 40 h to the temperature of 1200°C. Various cooling rates and thermal after-treatments following the diffusion step were applied. Besides the samples made in the own laboratory several zinc doped samples were used which were obtained from H. Mehrer and co-workers of the University of Münster, FRG, and from G. Pensl and co-workers of the University of Erlangen, FRG. Typical sample dimensions were 15 × 1.5 × 1.5 mm^3.

Measurements of electron paramagnetic resonance were performed at X-band (microwave frequency $\nu \cong 9$ GHz) and K-band ($\nu \cong 23$ GHz). Spectrometers were of the superheterodyne type with audio-frequency modulation of the magnetic field. The dispersion part of the magnetic susceptibility was observed at microwave power levels of a few microwatts. Samples were mounted with their crystallographic [0 $\bar{1}$ 1] direction vertically in the cylindrical cavity, perpendicular to the field of rotation of the magnetic field. Sample temperature during EPR experiment was 4.2 K, or within a few degrees above.

3. MAGNETIC RESONANCE SPECTRA

In this section the description of five new electron paramagnetic resonance spectra will be given.

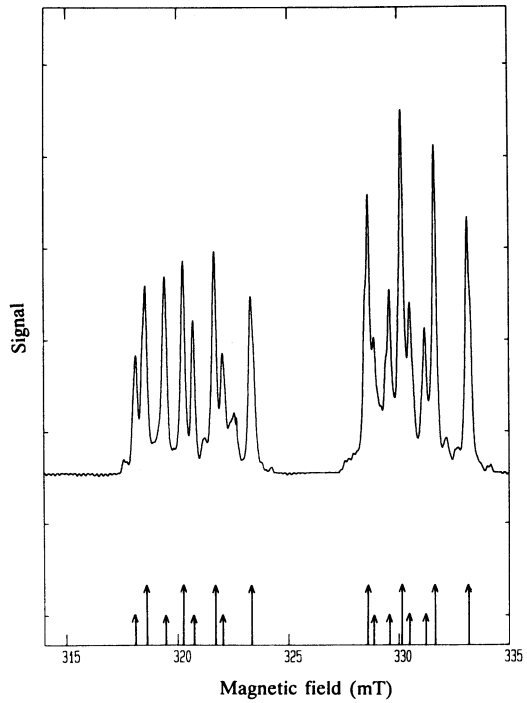

Fig. 1. Electron paramagnetic resonance spectrum of the Si:ZnCu centre, observed at temperature T = 4.2 K for magnetic field **B** ∥ [0 1 1], microwave frequency $\nu \cong 9$ GHz.

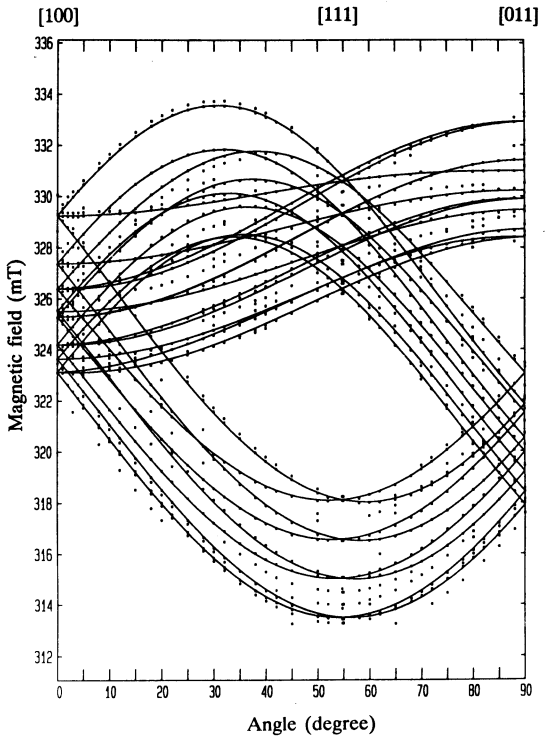

Fig. 2. Angular variation for the Si:ZnCu spectrum (Si-NL34) of the resonance fields (X-band) for rotation of the magnetic field in the (0 $\bar{1}$ 1) plane from [1 0 0] to [0 1 1]. Solid curves computed for the isotope ^{63}Cu.

3.1. *EPR spectrum Si-NL34*

A prominent spectrum was observed in *n*-type, phosphorus doped, and p-type, boron doped silicon of low ($\rho \cong 1$ Ohm cm) and high ($\rho \cong 1000$ Ohm cm) resistivity, of different origins. The spectrum measured in X-band for magnetic field parallel to [0 1 1] is shown in Fig. 1. Both groups of resonances, the one at the lower fields (318 mT < B < 324 mT) as well as the one at the higher fields (328 mT < B < 333 mT), consist of two quartets of lines. Measurement of the same spectrum in K-band revealed that the field splittings between the quartets were proportional to the frequency, whereas the splittings within the quartets were independent of frequency. The spectrum is thus understood to consist of 4 fine structure components each showing a 4 line hyperfine structure. The angular dependence of the observed spectrum for **B** in the (0 $\bar{1}$ 1) plane is shown in Fig. 2. All features of the rotation pattern, such as number of lines, their coincidences at high-symmetry directions and relative intensities, are characteristic for a centre with monoclinic-I symmetry.

The hyperfine splitting of all intensity into 4 equal-intensity components indicates the presence of one nucleus with spin I = 3/2 and 100% abundance. However, a careful inspection of the spectrum as given in Fig. 1 reveals that most lines have a shoulder on one side. This line shape is most pronounced on the outer lines of the quartets and the lower intensity shoulder is on the outside as measured from the centre of the quartet. A careful recording of the line shape for **B** ∥ [0 1 1] is shown in Fig. 3. The decomposition of the line into two components, indicated by the dashed Lorentzians, shows an intensity ratio near 2.4 for the two isotopes. The only element with two isotopes, of about 70% and 30% abundance, and each having I = 3/2, is copper. The splitting away from the centre of the quartet is 2.26 mT and 2.41 mT for the 70% and 30% abundant isotopes, respectively. The ratio 0.94 perfectly matches the ratio of the nuclear *g*-factors of the ^{63}Cu and ^{65}Cu isotopes. The conclusion that one copper atom is incorporated in the centre thus explains both intensity ratio and shift between the two spectral components.

To examine the participation of zinc in the centre a sample diffused with zinc, enriched to 91.9% in the isotope ^{67}Zn was prepared. A spectrum measured in such sample, compared with the similar spectrum for a sample with zinc of the natural composition, is given in Fig. 4. Even when not adequately resolved, the additional hyperfine structure due to the ^{67}Zn, with nuclear spin I = 5/2, is unmistakable.

Table 1. Spin Hamiltonian constants of the monoclinic-I centre Si: ZnCu (spectrum Si-NL34)

Spin S	Principal g-values			Direction θ	Remarks
	g_1	g_2	g_3		
1/2	1.9980	2.0872	1.9912	32.2	$g_1 \parallel [0\,1\,1]$ θ angle (g_3, [1 0 0])
Spin I	Principal A-values			Direction θ	Remarks
	A_1	A_2	A_3		
3/2	21.2	37.5	53.0	6.0	Isotope ^{63}Cu A-values in MHz

The quantitative analysis of the spectrum is based on the spin Hamiltonian $\mathcal{H} = +\mu_B \mathbf{B} \cdot \ddot{\mathbf{g}} \cdot \mathbf{S} + \mathbf{S} \cdot \ddot{\mathbf{A}} \cdot \mathbf{I}$, with electron spin $S = 1/2$ and nuclear spin $I = 3/2$. The solid lines in Fig. 2 are obtained from the computerized least squares fit, but are drawn only for the most abundant of the copper isotopes (^{63}Cu). Additional resonances corresponding with $\Delta m_I \neq 0$ transitions were occasionally observable. For further reference the spectrum is labelled Si-NL34. The constants as determined for the g and A tensors are given in Table 1.

3.2. *EPR spectrum Si-NL35*

Another prominent spectrum was observed in several samples, both with n- and p-type dopants. The spectrum arises from a trigonal centre, as demonstrated by the rotation pattern measured in X-band, shown in Fig. 5. Due to the large anisotropy and a small misorientation of the sample all four $\langle 1\,1\,1 \rangle$ orientations of the centre are separately visible in the spectrum. The angular dependence can be adequately analysed using the Hamiltonian $\mathcal{H} = +\mu_B \mathbf{B} \cdot \ddot{\mathbf{g}} \cdot \mathbf{S}$ and effective spin $S = 1/2$. The resulting values for the parallel and perpendicular principal values of the **g**-tensor are given in Table 2. From the value $g_\perp = 3.9980$ one concludes that the doublet in which the resonance is measured actually forms part of a spin quartet split into two doublets by a crystal field. To check further on this aspect the spectrum was also measured at the higher K-band frequencies. Also these measurements can be analysed with the effective spin $S = 1/2$ of the ground state doublet, though the fit is of less satisfactory quality; for the results see Table 2. The significantly lower value for $g_\perp$ at K-band as compared to X-band indicates that the splitting between the doublets is not very large compared to the microwave energy quantum. Therefore, X- and K-band data together were analysed with spin $S = 3/2$ and the Hamiltonian $\mathcal{H} = +\mu_B \mathbf{B} \cdot \ddot{\mathbf{g}} \cdot \mathbf{S} + D\{S_z^2 - S(S+1)/3\}$. In this way the experimental data could be fitted best and the physically more meaningful parameters $g_\parallel \cong g_\perp \cong 2$ for the g-values were obtained. The splitting 2D between the doublets is determined to be $\cong 140$ GHz.

A recorder trace of the spectrum for $\mathbf{B} \parallel [0\,1\,1]$ measured in X-band is shown in Fig. 6. Hyperfine structure due to silicon, isotope ^{29}Si, is clearly visible

Table 2. Spin Hamiltonian constants of the trigonal centre Si: ZnCr (spectrum Si-NL35)

Spin S	Principal g-values		D	Remarks
	$g_\parallel$	$g_\perp$		
1/2	1.9980	3.9980		X-band data
1/2	2.0016	3.9843		K-band data
3/2	1.9972	2.0004	70.6	X- and K-band data D-value in GHz
Spin I	Principal A-values ($S = 3/2$)			Remarks
	$A_\parallel$	$A_\perp$		
3/2	40.0	32.4		isotope ^{53}Cr A-values in MHz

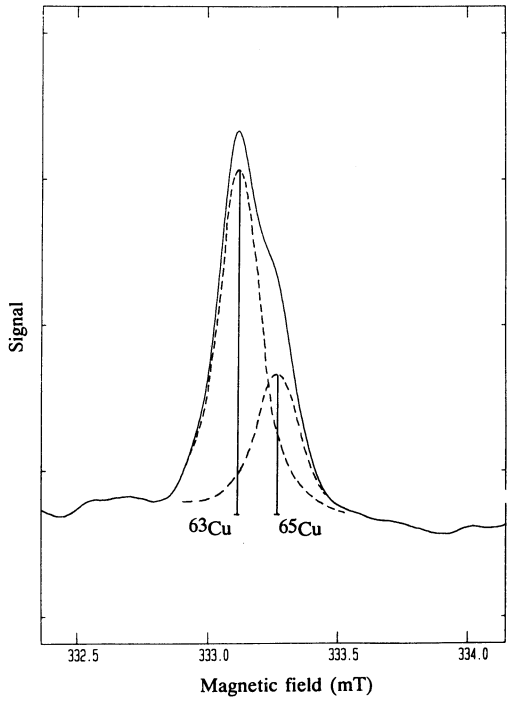

Fig. 3. Line shape of an $m_I = 3/2$ transition of the EPR of Si : ZnCu, observed for **B** ∥ [0 1 1]. The partially resolved hyperfine splitting due to the ^{63}Cu and ^{65}Cu isotopes is shown.

very near the central lines. In addition a structure of four equidistant small satellites is observed, apparently corresponding to an $I = 3/2$ nucleus. From the relative intensities of the lines the abundance of the isotope is estimated at about 9%. The natural candidate then is the ^{53}Cr isotope. The full angular dependence of the splitting could be measured and analysed. In Fig. 7 the experimental data points and the computed curves, following least squares matching schemes, are represented. Table 2 gives the values of the constants of the trigonal hyperfine tensor. Although this interpretation appears to be secure, the possibility that the quartet of lines is actually composed of two doublets associated with two ^{29}Si shells cannot absolutely be discarded. Further measurements with controlled enriched ^{53}Cr doping will clarify on this point.

Also for this spectrum the presence of zinc in the centre was verified by doping with ^{67}Zn. The positive conclusion is corroborated by the additional hyperfine structure observed in such samples. The result as presented in Fig. 8 shows that in this case the structure is not the simplest 6 equidistant lines. For the value $I = 5/2$ of ^{67}Zn interactions of higher order in I, such as quadrupole interactions, may be important. The quantitative analysis is not available at this instance.

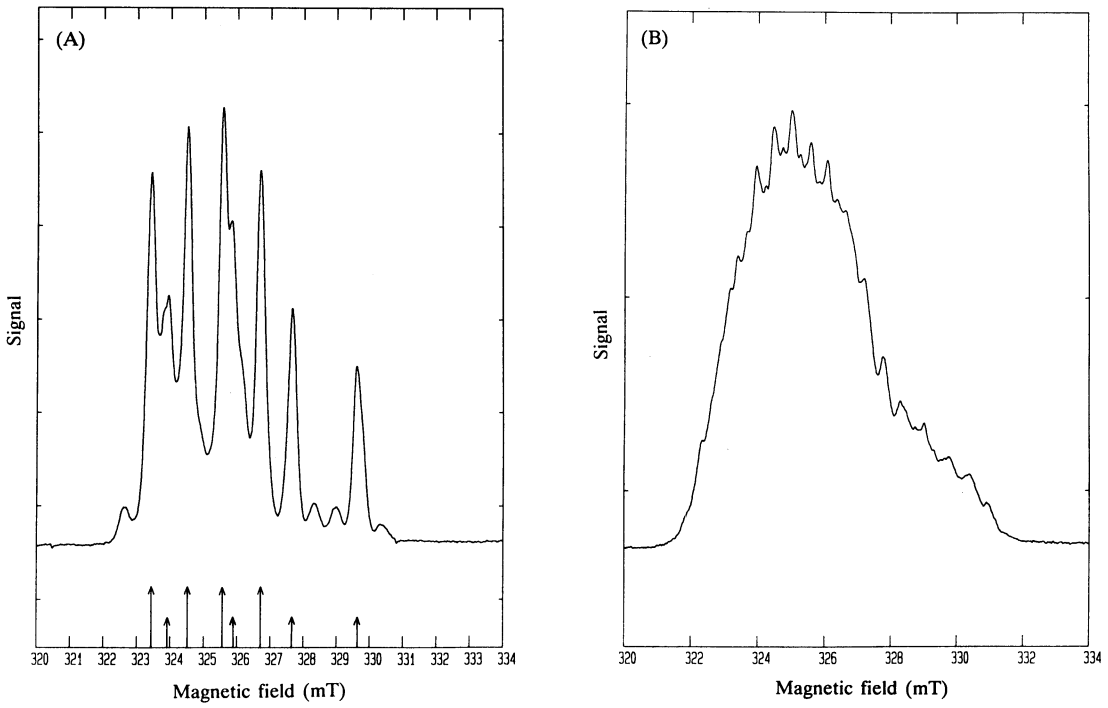

Fig. 4. EPR spectrum of the Si : ZnCu centre after diffusion with (A) zinc of the natural isotopic composition, and (B) with zinc enriched to 91.9% in the isotope ^{67}Zn with nuclear spin $I = 5/2$. Magnetic field **B** ∥ [1 0 0], microwave frequency $\nu \cong 9$ GHz.

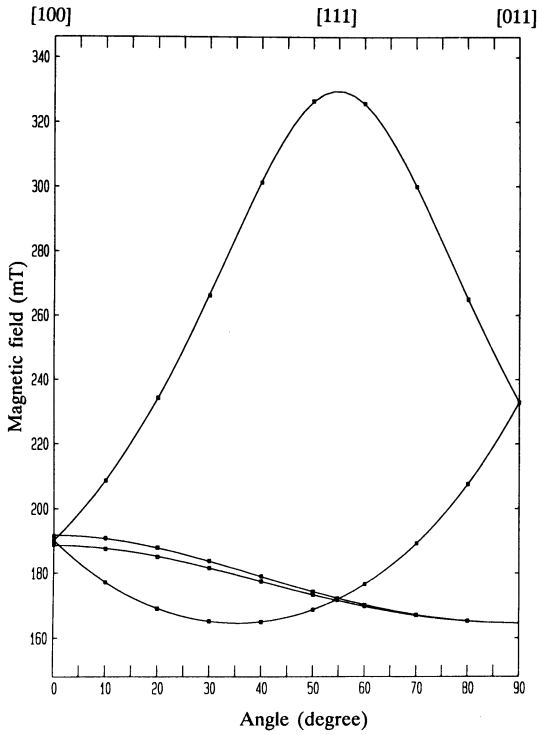

Fig. 5. Angular variation for the Si : ZnCr spectrum (Si-NL35) of the resonance fields (X-band) for rotation of the magnetic field in the (0 $\bar{1}$ 1) plane from [1 0 0] to [0 1 1]. Solid curves computed with the small misorientation taken into account.

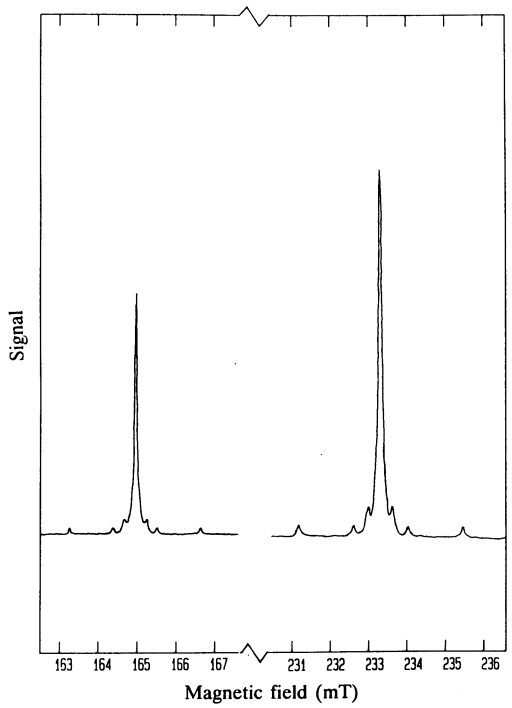

Fig. 6. Electron paramagnetic resonance spectrum of the Si : ZnCr centre, observed at temperature T = 4.2 K for magnetic field **B** ∥ [0 1 1], microwave frequency $\nu \cong 9$ GHz. Fourfold splitting due to hyperfine interaction with ^{53}Cr isotope, natural abundance 9.54%, is observable.

3.3. *EPR spectrum Si-NL36*

This spectrum was observed in a high resistivity *p*-type, boron doped, sample. It was observed after illumination with white or sub-bandgap light. The symmetry of the corresponding centre is orthorhombic-I. The parameters of the spin Hamiltonian analysis with Zeeman energy term and spin $S = 1/2$ are given in Table 3.

3.4. *EPR spectrum Si-NL37*

This is another spectrum found in the high resistivity *p*-type material. Also for observation of this spectrum the illumination of the sample was required. The symmetry of the centre is monoclinic-I. Parameters of the analysis are given in Table 3, with the same definition for the orientation angle θ as for spectrum NL34.

3.5. *EPR spectrum Si-NL38*

Measurements in an *n*-type sample, phosphorus doped, resistivity 1 Ohm cm, revealed this spectrum, requiring no illumination. It corresponds to a centre of trigonal symmetry. For the same reasons as discussed for spectrum NL35 the spin Hamiltonian analysis required an effective spin $S = 3/2$. The parameters for the Zeeman energy tensor $\tilde{\mathbf{g}}$ and for the crystal field term D are reported in Table 3. The doublet splitting is apparently quite small. Presumably, the

Table 3. Spin Hamiltonian constants of EPR spectra observed in zinc doped silicon

Spectrum	Symmetry	Spin S	Principal g-values			Direction θ	Remarks
			g_1	g_2	g_3		
Si-NL36	Orthorhombic-I	1/2	1.9856	1.9903	2.0119		g_1 ∥ [1 0 0]
Si-NL37	Monoclinic-I	1/2	2.0164	2.0507	1.9981	43.4	g_1 ∥ [0 1 1]
Si-NL38	Trigonal	3/2	2.1520	2.0328	2.0328		g_1 ∥ [1 1 1] D = 15.9 GHz

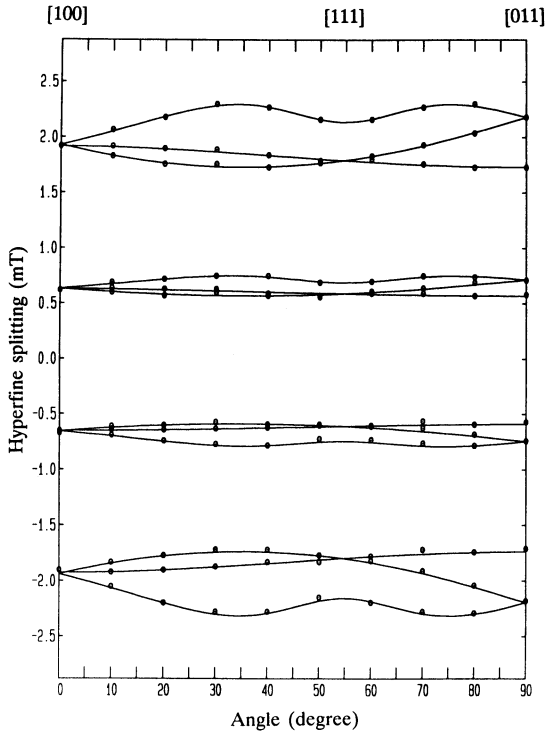

Fig. 7. Angular variation of the hyperfine splitting by the ^{53}Cr isotope in the Si : ZnCr centre for rotation of **B** in the (0 $\bar{1}$ 1) plane. Experimental data points: ○; solid curves computed result for $m_I = +3/2, +1/2, -1/2$ and $-3/2$.

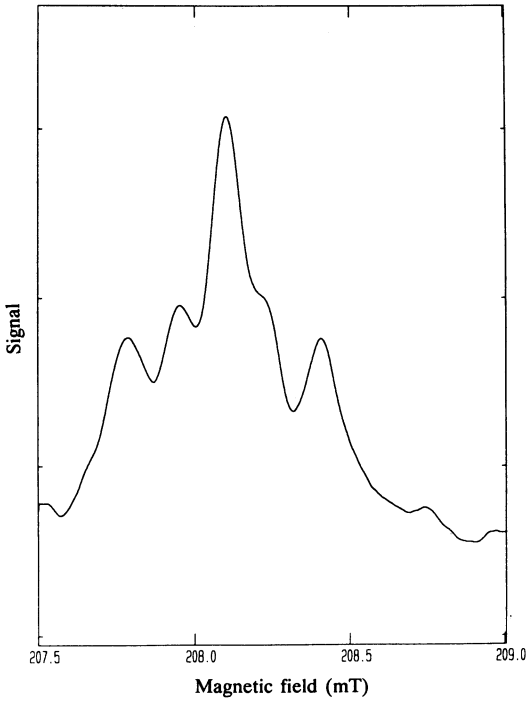

Fig. 8. EPR spectrum of the Si : ZnCr centre after diffusion with zinc enriched to 91.9% in the isotope ^{67}Zn (nuclear spin $I = 5/2$), leading to non-equidistant splitting between the hyperfine lines. Magnetic field **B** 80° away from [1 0 0], microwave frequency $\nu \cong 9$ GHz.

centre is iron related. Several arguments support this preliminary presumption. The spectrum was not present in the sample immediately after its preparation by diffusion. Only after storing the sample some months at room temperature the spectrum was present. The spectrum due to neutral interstitial iron was also observed in this sample. The positive deviation of the g-value from $g = 2$ by 0.05 to 0.1 is common for iron related centres. Finally weak structure possibly arising from the isotope ^{57}Fe, in its natural abundance of 2.2%, seemed to be present. Samples with enriched ^{57}Fe will be prepared to check on this point. The spectrum is rather similar to Si-A22 [13], but according to the present analysis the parameters of the two spectra are different outside experimental error.

Acknowledgements – The authors are grateful to G. Pensl, P. Stolz and M. Lang of the University of Erlangen, Germany, and H. Mehrer, N.A. Stolwijk and D. Grünebaum of the University of Münster, Germany, for stimulating discussions and for providing many samples. The work received financial support from the Foundation for Fundamental Research on Matter (FOM).

REFERENCES

1. C.S. Fuller & F.J. Morin, *Phys. Rev.* **105,** 379 (1957).
2. R.O. Carlson, *Phys. Rev.* **108,** 1390 (1957).
3. H. Lemke, *Phys. Status Solidi* (*a*) **72,** 177 (1982).
4. P. Stolz, G. Pensl, D. Grünebaum & N. Stolwijk, *Mater. Sci. Eng. B* **4,** 31 (1989).
5. S. Weiss, R. Beckmann & R. Kassing, *Appl. Phys. A* **50,** 151 (1990).
6. B.V. Kornilov, *Sov. Phys. – Solid State* **5,** 2420 (1964).
7. E. Merk, J. Heyman & E.E. Haller, *Solid State Commun.* **72,** 851 (1989).
8. A. Dörnen, R. Kienle, K. Thonke, P. Stolz, G. Pensl, D. Grünebaum & N.A. Stolwijk, *MRS Symp. Proc.*, Boston (1989).
9. J.M. Hermann, III & C.T. Sah, *Phys. Status Solidi* (*a*) **14,** 405 (1972).
10. G.W. Ludwig & H.H. Woodbury, *Solid State Phys.* **13,** 223 (1962).
11. M. Lang, private communication (1990).
12. V.B. Ginodman, P.S. Gladkov, B.G. Zhurkin & B.V. Kornilov, *Sov. Phys. – Semicond.* **5,** 1930 (1972).
13. Y.H. Lee, R.L. Kleinhenz & J.W. Corbett, *Defects and Radiation Effects in Semiconductors* 1978, p. 521. Institute of Physics, Bristol (1979).